AGU PUBLICATIONS

Geophysical Research Letters

RESEARCH LETTER
10.1002/2017GL075807

Key Points:
- Thermodynamic and dynamic effects on the mean circulation create wet Last Glacial Maximum (LGM) in western North America
- Transient eddies do not make a significant contribution to pluvial conditions at LGM
- These conclusions hold across a strong spatial gradient in precipitation seasonality

Supporting Information:
- Supporting Information S1

Correspondence to:
C. Morrill,
carrie.morrill@colorado.edu

Citation:
Morrill, C., Lowry, D. P., & Hoell, A. (2018). Thermodynamic and dynamic causes of pluvial conditions during the Last Glacial Maximum in western North America. *Geophysical Research Letters*, *45*, 335–345. https://doi.org/10.1002/2017GL075807

Received 3 OCT 2017
Accepted 27 NOV 2017
Published online 9 JAN 2018

Thermodynamic and Dynamic Causes of Pluvial Conditions During the Last Glacial Maximum in Western North America

Carrie Morrill[1,2], Daniel P. Lowry[2,3], and Andrew Hoell[4]

[1]Cooperative Institute for Research in Environmental Sciences, University of Colorado Boulder, Boulder, CO, USA, [2]NOAA's National Centers for Environmental Information, Boulder, CO, USA, [3]Now at Victoria University of Wellington, Wellington, New Zealand, [4]Physical Sciences Division, NOAA/Earth System Research Laboratory, Boulder, CO, USA

Abstract During the last glacial period, precipitation minus evaporation increased across the currently arid western United States. These pluvial conditions have been commonly explained for decades by a southward deflection of the jet stream by the Laurentide Ice Sheet. Here analysis of state-of-the-art coupled climate models shows that effects of the Laurentide Ice Sheet on the mean circulation were more important than storm track changes in generating wet conditions. Namely, strong cooling by the ice sheet significantly reduced humidity over land, increasing moisture advection in the westerlies due to steepened humidity gradients. Additionally, the removal of moisture from the atmosphere by mass divergence associated with the subtropical high was diminished at the Last Glacial Maximum compared to present. These same dynamic and thermodynamic factors, working in the opposite direction, are projected to cause regional drying in western North America under increased greenhouse gas concentrations, indicating continuity from past to future in the mechanisms altering hydroclimate.

1. Introduction

The southwestern United States (SW U.S.) is the most arid region of the country, and any future changes in water availability will have important consequences for human and other natural systems. Understanding the causes of past hydrologic extreme periods may help to clarify possible future changes. One of the most significant past hydrologic changes occurred at the Last Glacial Maximum (LGM) (~21,000 years ago, or 21 ka). During the LGM, many currently dry catchments in the SW U.S. were filled with permanent lakes tens to hundreds of meters deep (Mifflin & Wheat, 1979; Reheis et al., 2014). Additional proxy evidence for pluvial conditions exists from the geochemistry of cave deposits (Asmerom et al., 2010; Wagner et al., 2010) and of pedogenic opal (Maher et al., 2014), as well as vegetation assemblages preserved in packrat middens (Oster et al., 2015).

It has been hypothesized that the wet conditions during the LGM were caused by a strengthened and southward displaced jet stream forced by the Laurentide Ice Sheet (LIS) into the SW U.S. (Antevs, 1948; COHMAP members, 1988). This hypothesis has been supported by model simulations of the LGM (COHMAP members, 1988). However, new proxy evidence for dry glacial conditions in coastal California (Lyle et al., 2012) and for synchrony of lake high stands across the SW U.S. (Ibarra et al., 2014; Munroe & Laabs, 2013) now questions the jet stream hypothesis, by contradicting the latitudinal banding of moisture anomalies expected from Pacific-sourced storms and the time-transgressive pattern of lake level change predicted from northward retreat of the storm track as the LIS melted.

Extensions and alternatives to the jet stream hypothesis have been proposed to explain these more complex patterns of moisture anomalies from the last glacial period. One study found that a meridionally compressed and northwest-southeast trending jet stream best explains observed LGM moisture patterns (Oster et al., 2015). Other alternative explanations invoke a southerly rather than westerly source of glacial precipitation (Lyle et al., 2012), intensified and southward shifted atmospheric rivers (Lora et al., 2017), or an inverse application of the "wet get wetter, dry get drier" phenomenon proposed for future climate, whereby cooling causes existing patterns of atmospheric moisture divergence and convergence to weaken (Boos, 2012; Quade & Broecker, 2009). Past attempts to test these hypotheses have focused strictly on either dynamic

aspects of the flow or thermodynamic scaling of temperature changes and are unable to provide insight into their relative importance.

Here we use state-of-the-art coupled climate model simulations of the LGM and preindustrial (PI) (1750 A.D.) periods to provide the first full accounting of both dynamic and thermodynamic causes of atmospheric moisture variations. Employing the atmospheric moisture budget calculation of Seager et al. (2010), we identify the factors responsible for moisture convergence in the atmosphere that balance the net precipitation-evaporation (*P-E*) flux to/from the land surface.

2. Materials and Methods

We analyzed nine simulations completed for the Coupled Model Intercomparison Project phase 5/Paleoclimate Modeling Intercomparison Project phase 3 (CMIP5/PMIP3) (Table S1 in the supporting information; Braconnot et al., 2012). These simulations were completed at varying resolutions, and their boundary conditions generally followed PMIP3 protocols with a few exceptions (Text S1). We also analyzed 100 years of a sensitivity experiment completed with the Community Climate System Model, version 4 (CCSM4), in which CO_2 concentrations were set to LGM values while all other boundary conditions altered in the CCSM4 CMIP/PMIP experiment (i.e., orbital forcing, ice sheets, sea level, CH_4, and N_2O) were set to PI values (Brady et al., 2013). Brady et al. (2013) estimated that decreased CO_2 and the LIS yield the most important global mean radiative forcings in their CCSM4 LGM experiments (each about -2.7 W/m^2). Radiative forcing from surface albedo changes caused by sea level fall were significantly smaller (about -0.8 W/m^2), while orbital forcing and non-CO_2 greenhouse gases were even less potent (Yoshimori et al., 2009). Given this information and the likely strong regional effects of the LIS on western North America, we considered that comparing results from the CO_2-only simulation, termed LGM_{CO2}, to the CMIP/PMIP experiments, termed LGM_{ALL}, primarily indicated the effects of the LIS.

We performed an atmospheric moisture budget analysis using 100 years of monthly, pressure-level output from each of the CMIP/PMIP model simulations. The moisture budget equation can be written as (e.g., Seager et al., 2010)

$$\rho_w g(P-E) = -\int_0^{p_s} (\overline{u}\cdot\nabla\overline{q} + \overline{q}\nabla\cdot\overline{u})\mathrm{d}p - \int_0^{p_s} \nabla\cdot\left(\overline{u'q'}\right)\mathrm{d}p - q_s u_s\cdot\nabla p_s \quad (1)$$

where p is pressure, q is specific humidity, u is the horizontal vector wind, ρ_w is the density of water, the subscript s specifies surface values, overbars specify monthly means, and primes specify departures from monthly means. The moisture budget in equation (1) states that precipitation minus evaporation from the land surface is balanced by moisture convergence by atmospheric mean flow expressed as the sum of two components representing advection and divergent flow (first integral), moisture convergence by transient eddies (second integral), and a boundary term that represents flow of moisture along surface pressure gradients (third term).

We applied a methodology from Seager et al. (2010) to further break down the advection and divergent flow terms for each individual model into their thermodynamic and dynamic components, where the thermodynamic component is related to changes in q and the dynamic component is related to changes in u. By setting q to LGM-PI anomaly values and holding u constant at PI values, we estimated the thermodynamic contributions to the advection term (ADV_{TD}) and the divergent flow term (DIV_{TD}). By setting u to LGM-PI anomaly values and holding q constant at PI values, we estimated the dynamic contributions to the advection term (ADV_D) and the divergent flow term (DIV_D):

$$\delta\mathrm{ADV}_{\mathrm{TD}} = -\int_0^{p_s} (\overline{u}_{\mathrm{PI}}\cdot\nabla\delta\overline{q})\mathrm{d}p \quad (2)$$

$$\delta\mathrm{DIV}_{\mathrm{TD}} = -\int_0^{p_s} (\delta\overline{q}\nabla\cdot\overline{u}_{\mathrm{PI}})\mathrm{d}p \quad (3)$$

$$\delta\mathrm{ADV}_{\mathrm{D}} = -\int_0^{p_s} (\delta u\cdot\nabla\overline{q}_{\mathrm{PI}})\mathrm{d}p \quad (4)$$

$$\delta\mathrm{DIV}_{\mathrm{D}} = -\int_0^{p_s} (\overline{q}_{\mathrm{PI}}\nabla\cdot\delta\overline{u})\mathrm{d}p \quad (5)$$

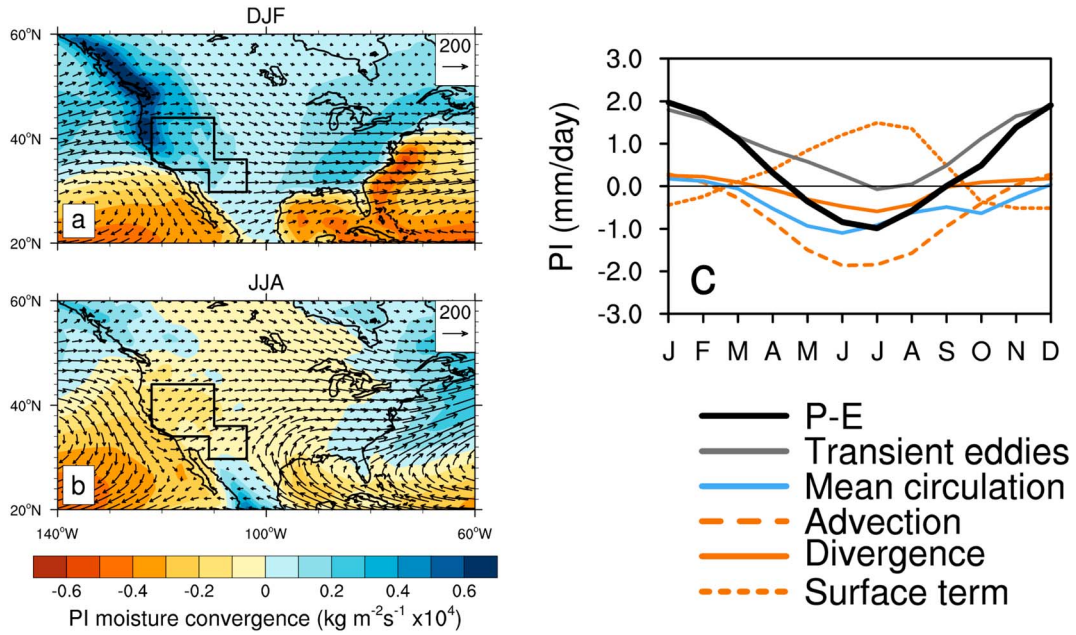

Figure 1. Vertically integrated moisture convergence (shading, kg m^{-2} s^{-1} × 10^{-4}) and vertically integrated moisture transport (vectors, in kg m^{-1} s^{-1}) for (a) December–January–February and (b) June–July–August in the CMIP/PMIP multimodel preindustrial ensemble. Polygon outlined in black shows the area averaged for (c) the annual cycle of atmospheric moisture budget terms.

where the subscript PI denotes mean preindustrial values and δ indicates the change from LGM to PI. The total thermodynamic contribution was calculated as the sum of δADV_{TD} and δDIV_{TD}, and the total dynamic contribution was calculated as the sum of δADV_{D} and δDIV_{D}.

We are unable to calculate the transient eddy flux directly, given that only monthly outputs of the variables necessary for the moisture budget analysis have been archived for the CMIP/PMIP simulations. Instead, we calculated *P-E* and moisture convergence by the mean circulation (i.e., the divergence of the vertical integral of moisture transport), and then computed the transient eddy flux as a residual, as done successfully in previous studies (e.g., Wills et al., 2016). The CMIP/PMIP model output is available only on pressure levels; thus, we used the methodology presented in section 5 of Seager and Henderson (2013) to calculate the integrals in the first term of equation (1) and in equations (2)–(5) given that the lower limits of integration are different by grid cell due to varying surface pressure. Following the recommendation of Seager and Henderson (2013), we calculated the surface term as the difference between the divergence of the vertical integral of moisture transport and the vertical integral of the divergence of moisture transport. We also applied a barotropic correction to the zonal and meridional winds at each atmospheric level to minimize the mass budget residual. For all plots showing multimodel ensemble means, we used bilinear interpolation to convert each model's values to a 1° × 1° grid and then computed a simple average of all nine models.

To verify the models' ability to realistically simulate LGM moisture conditions, we qualitatively compared model output with paleoclimate indicators of precipitation-evaporation. We have primarily focused on lake level reconstructions from closed-basin lakes, which are the most spatially complete and best dated proxy comparison to model *P-E*. We used age-controlled lake level information from 16 lake basins to verify LGM age (defined as 19–23 ka) for past lake shorelines (Table S2). All radiocarbon-dated shorelines have been calibrated using Calib 7.1 (Stuiver & Reimer, 1993) and IntCal13 (Reimer et al., 2013), with the 2 sigma error range reported in Table S2.

By definition, however, *P-E* averaged over a closed basin in hydrologic steady state is 0, complicating our use of lake level information to gauge changes in *P-E* through time (Broecker, 2010). There are several pieces of evidence for positive *P-E* anomalies at LGM compared to preindustrial, however. First, the two most temporally complete lake level records, from Bonneville and Surprise, show rising lake levels through the LGM (Ibarra et al., 2014; McGee et al., 2012; Oviatt, 2015). This indicates that lakes were not in steady state and

that anomalous moisture convergence relative to PI occurred. Additionally, there is good evidence that surface infiltration, water tables, and groundwater recharge rates were higher across the southwest United States at the LGM compared to present based on pedogenic opal (Maher et al., 2014), spring and wetland deposits (Quade et al., 2003), fossil groundwater (Kulongoski et al., 2009; Zhu et al., 1998), and speleothems (Musgrove et al., 2001; Szabo et al., 1994). These are all further indications of net gain in water balance (*P-E*) in the region at the LGM compared to present.

3. Results

In general, the CMIP/PMIP models reproduce important aspects of present-day hydroclimate in the SW U.S. (cf. Figures 1 and S1 and Figures 1 and 2 in Seager et al., 2014). Today, the SW U.S. experiences an arid to semiarid climate with annually averaged precipitation-evaporation (*P-E*) values ~0.1 mm/day. The region has a strong seasonal cycle in its atmospheric water budget, with moisture convergence in the winter and moisture divergence in the summer (Figures 1a and 1b). Transient eddies converge moisture to the SW U.S., while moisture advection and, to a lesser extent, the divergent component of the mean circulation that is associated with subsidence in the subtropical high dry the atmosphere. The surface term, representing the flow of moisture down pressure gradients, is also important in summer providing a wetting that counteracts the drying tendency of advection.

Likewise, the CMIP/PMIP multimodel ensemble produces increased annual *P-E* across the SW U.S. at LGM compared to PI (Figure 2a), as expected from proxy records. Coherency among the individual models in the sign of the annual *P-E* anomaly is high (Figure S2). For the multimodel ensemble mean, *P-E* is increased at LGM compared to PI in all months, though variability exists among models regarding the seasonality of greatest *P-E* change (Figure 3).

Our moisture budget analysis using the CMIP/PMIP output suggests that mean circulation is more important than transient eddies or the surface term in causing increased annual *P-E* (Figure 2a) at the LGM across the SW U.S. (cf. Figures 2b, 2c, and 2e). In the multimodel ensemble, moisture convergence by transient eddies weakens at the LGM across most of the study area, although the surface term shows some potential localized contribution to moisture convergence. Even though fewer than seven of nine models agree on the direction of change at the grid cell level for some moisture budget components (Figure 2), this threshold is generally met or exceeded when components are averaged over the western North America polygon shown in Figure 1 (Figure S3).

The CMIP/PMIP models, as documented by Oster et al. (2015), consistently simulate a stronger winter jet stream over western North America but disagree regarding whether the jet was shifted southward. These authors have also shown that the few CMIP/PMIP models with archived daily data simulate stronger and southward shifted eddy energy (i.e., perturbations in the zonal and meridional wind speed) for the SW U.S. at the LGM relative to PI. However, our assessment of the moisture converged by these wind speed perturbations, considering thermodynamics in addition to dynamics in the same simulations, does not support transient fluxes as a direct cause of higher *P-E* at the LGM. We infer that thermodynamical factors outweigh dynamical factors in determining moisture convergence by transient eddies at LGM.

We divide changes in the mean circulation into dynamic (atmospheric motions) and thermodynamic (moisture distribution) components, showing that aspects of both thermodynamics and dynamics contribute to differences between LGM and PI (Figures 2f–2i and 3). The thermodynamic effect is driven by colder temperatures at the LGM that, assuming a constant relative humidity, reduce the specific humidity of the atmosphere according to the Clausius-Clayperon relationship. Further dividing the thermodynamic effect into its two subcomponents, that is, reflecting changes in the specific humidity gradient (i.e., δADV_{TH}) and changes in the specific humidity being diverged/converged (i.e., δDIV_{TH}), shows that the former yields a greater contribution (Figures 2f and 2h). The change in the specific humidity gradient occurs due to greater cooling toward the LIS at the LGM, leading to a weakened (strengthened) humidity gradient in summer (winter) when advection is drying (wetting). Thus, moisture advection by the mean westerlies is enhanced in both seasons, with maximum anomalies centered on the 700 mbar level (Figures S4 and S5). This effect is weakest in the winter across most of the models (Figure 3), reflecting the fact that the smallest absolute change in specific humidity gradient occurs during the coldest season of the year. Wind speeds slow from winter to spring and summer, but this effect on moisture advection is diminished by the fact that wind vectors near the 700 mbar level also shift

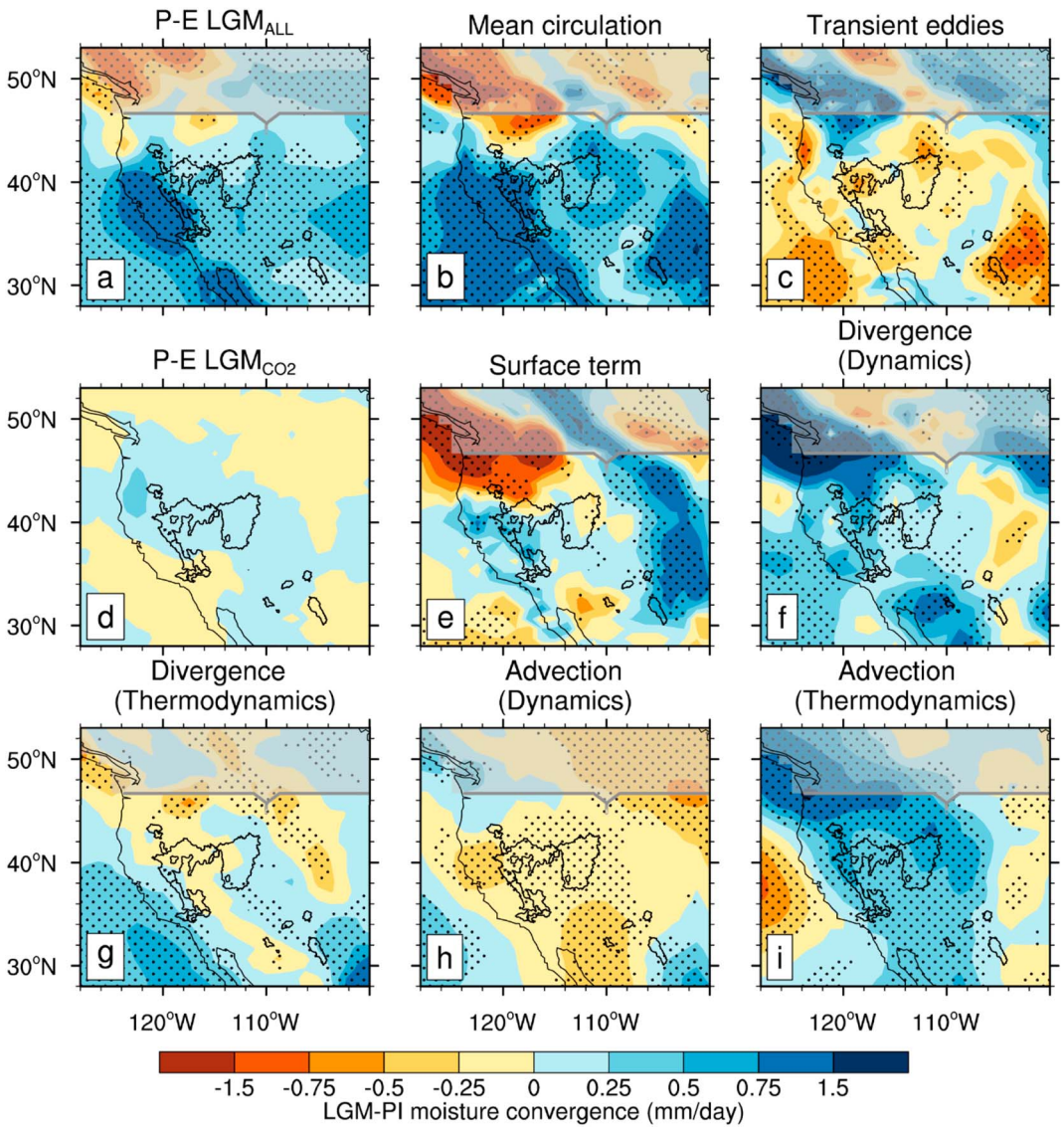

Figure 2. Annual mean atmospheric moisture budget component anomalies for CMIP/PMIP multimodel ensemble LGM experiments compared to PI. (a) Precipitation minus evaporation for LGM_{ALL} experiments, which incorporate LGM orbital forcing, greenhouse gas concentrations, ice sheets, and sea level change. (b) Moisture convergence by the mean circulation in LGM_{ALL}. (c) Moisture convergence by transient eddies in LGM_{ALL}. (d) Precipitation minus evaporation for the LGM_{CO2} simulation completed with the CCSM4, which incorporates LGM CO_2 levels with all other boundary conditions set to preindustrial values. (e) Moisture convergence by the surface term in LGM_{ALL}. (f–i) Dynamic and thermodynamic contributions to moisture convergence by the mean circulation in LGM_{ALL}. Stippling indicates agreement among at least seven of the nine models on sign of anomaly. Black lines show the drainage basins of lake level records listed in Table S2. The location of the LGM ice sheet is shown by semitransparent gray shading.

from westerly to southwesterly, becoming more perpendicular to specific humidity contours during this seasonal transition (Figures S5e–S5g).

Dynamic components of the changes in mean circulation moisture convergence include changes in the strength of the westerlies (δADV_D) and of the divergent circulation (δDIV_D; i.e., subtropical high and downwelling branch of the Hadley circulation). Further subdividing the dynamical contribution into these subcomponents (Figures 2f, 2h, and 3) clearly shows that the latter is critical for maintaining positive *P-E* anomalies at the LGM. This effect generally lasts year-round (Figure 3) and is associated with a weakening of subsidence and of the subtropical (North Pacific) high (Figure S6). This weakening of subsidence appears to be a

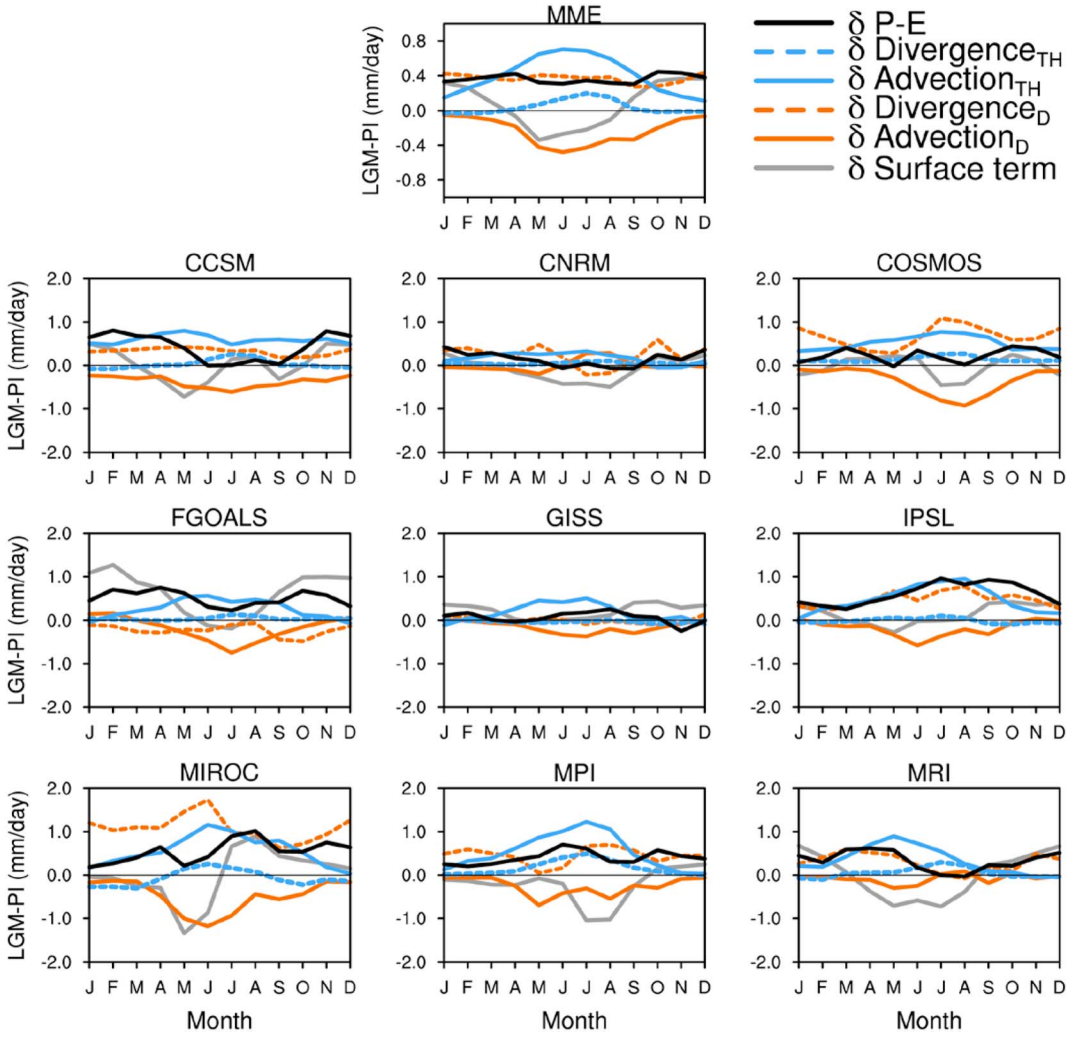

Figure 3. Seasonal cycle of anomalies (LGM_{ALL}-preindustrial) in the thermodynamic (TH) and dynamic (D) contributions to the mean circulation divergence and advection in the CMIP/PMIP multimodel ensemble and in the nine models that compose the ensemble. Values have been averaged over a polygon in western North America, as delineated in Figure 1.

regional phenomenon, as most other areas under the influence of subtropical highs experience increased subsidence at the LGM compared to PI (Figure S6), related to increased latitudinal temperature gradients and strengthening of the Hadley circulation (e.g., Otto-Bliesner & Clement, 2005). Indeed, analysis of a model participating in PMIP2 indicates that multiple factors probably weakened the North Pacific high at LGM; most importantly, the high albedo of the LIS reduced the land-ocean difference in diabatic heating in summer, and anomalies in the midlatitude SST gradient altered heat and momentum transport in the storm track in winter (Yanase & Abe-Ouchi, 2010).

Evidence for increased precipitation-evaporation at LGM compared to present exists across a broad climatic gradient defined by the seasonality of precipitation (Figures 4a and S7). It is noteworthy that the causes of anomalously positive atmospheric water budget during the LGM relative to PI do not vary substantially across this gradient. For both northern (more winter-dominated precipitation) and southern (less winter-dominated precipitation) subregions, mean circulation changes associated with weakening in the specific humidity gradient under constant relative humidity and in mass divergence are key contributors to anomalous moisture convergence at LGM (Figures 4b and 4c). One difference between these two regions is in the seasonality of the *P-E* anomalies. The Great Basin (north) experienced consistent, year-round *P-E* anomalies relative to PI times albeit with a peak during the summer half year caused by the thermodynamic component of

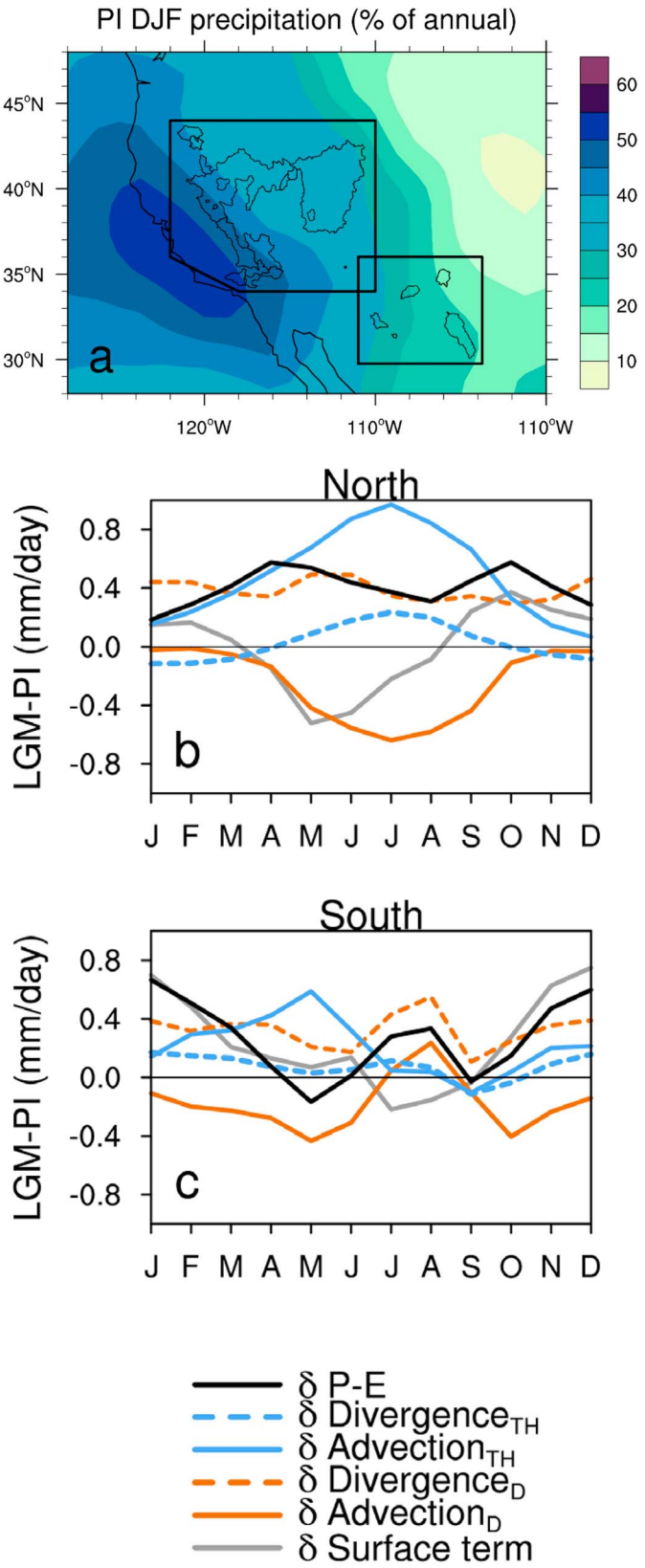

Figure 4. Subregional analysis of anomalous atmospheric moisture budget components. (a) The areal extent of the northern (more dominated by winter precipitation) and the southern (less dominated by winter precipitation) subregions shown with winter precipitation percentage calculated from the preindustrial CMIP/PMIP ensemble mean. LGM-PI budget components for the (b) northern and (c) southern subregions.

advection, while the south experienced peaks in both the summer monsoon and winter seasons relative to PI times. Another important difference between these regions is the relative importance of the surface term that, while difficult to interpret in a physical way, contributes significantly to anomalous moisture convergence during the winter in the south.

Lowered CO_2 levels contribute very little to moisture changes observed at the LGM, as shown by the LGM_{CO2} experiment (Brady et al., 2013) (Figure 2d). Rather, the LIS is the most likely source of the moisture budget changes at the LGM due to its extreme cooling effects on the mean circulation over North America. Thus, even if the transient eddy impacts of the ice sheet are secondary to its mean circulation effects in terms of creating wetter conditions in the western United States, increases in precipitation-evaporation at LGM would likely have been muted in the absence of the LIS.

4. Conclusions

We have identified aspects of mean circulation changes that are critical for generating pluvial conditions across the SW U.S. during the LGM using an ensemble of nine state-of-the-art climate models. Unlike previous explanations for LGM moisture that invoke a strengthening of processes that moisten the atmosphere in this part of the world (i.e., transient eddy activity), our results point to the importance of the weakening of processes that typically dry the atmosphere (i.e., mean moisture advection and the divergent circulation). In other words, gains to *P-E* during the LGM result partly from exporting less moisture from the SW U.S., not just importing more.

One caveat to this interpretation is that climatological shifts in transient eddy activity, as related to a storm track shift or to intensification of atmospheric rivers, will impact the mean climate. This is particularly true for western North America, where atmospheric rivers are an important source of moisture transport (Newman et al., 2012). In fact, Lora et al. (2017) have argued that the CMIP/PMIP ensemble indicates a southward shift and intensification of atmospheric rivers across the SW U.S. at LGM compared to PI. Our analysis cannot completely rule out a role for transient eddy activity in generating pluvial conditions at LGM, but this mechanism and the mean circulation changes that we describe do not have to be mutually exclusive. Several points emerge to argue for mean circulation changes playing an important role, either with or without other processes. First, changes in moisture convergence between LGM and PI due to the mean circulation are either similar (in the case of δDIV_D) or greater (in the case of δADV_{TD}) during summer relative to winter, the main season for transient eddy activity. Second, it is not too surprising that the large, mean state radiative forcing of the LIS and its impact on temperature gradients would be capable of generating the sort of changes in the mean circulation that we describe. Last, all models in the CMIP/PMIP ensemble generate positive LGM-PI *P-E* anomalies over the SW U.S., despite the fact that they vary significantly in the degree to which they simulate southward shifted storms (Lora et al., 2017). Future analyses with higher-temporal-resolution model output will be necessary to resolve these issues.

Our results have two important implications for understanding hydrologic variations in the SW U.S. First, we demonstrate that the PMIP subset of models being used to make future projections are successful in qualitatively capturing past known hydrologic variability in this region. Further work is necessary to determine whether these models quantitatively reproduce the size of the moisture changes, rather than just the spatial scale and the directional change. Additionally, other factors such as lake evaporation or precipitation recycling from large lakes, which are not captured by the CMIP/PMIP simulations due to their omission of pluvial lakes, can play an important role in determining lake level and the regional atmospheric water budget (Hostetler et al., 1994; Pound et al., 2014). Second, our results highlight the central role that mean circulation changes have played in determining *P-E* during the LGM; comparable hydrologic change is observed in lake and speleothem records during past glacial maxima, and the mechanisms outlined here could also be relevant for these changes (Lachniet et al., 2014; Oviatt et al., 1999). Other important findings from proxy records of the last glacial and deglaciation highlight temporal variability in hydroclimate that we have not been able to address using solely the CMIP/PMIP time slice ensemble, including the existence of lake highstands during deglaciation (Lora et al., 2016; Maher et al., 2014; Wong et al., 2016). Further analysis of the atmospheric water budget in transient simulations would test whether mean circulation changes explain this variability as well as they do the glacial mean state.

Future projections indicate that the SW U.S. will dry over the next century due to a combination of effects in the mean circulation, both thermodynamic and dynamic (Lau & Kim, 2015; Seager et al., 2014, 2007). Melting of the LIS during the last deglaciation is a fundamentally different climate forcing than increased anthropogenic atmospheric greenhouse gas concentrations, yet both apparently drive changes in the mass divergence (Lau & Kim, 2015) and in atmospheric humidity associated with a land-ocean warming contrast (Sutton et al., 2007). Thus, important parallels exist between past and future hydroclimate changes, though continued future impacts to the hydroclimate of the SW U.S. over the next century are likely to develop at a rate faster than that paced by the relatively slow, orbital-driven melting of the LIS.

Acknowledgments
We acknowledge the World Climate Research Programme's Working Group on Coupled Modeling and the Paleoclimate Modeling Intercomparison Project for CMIP/PMIP model output and NOAA/OAR/ESRL PSD for Livneh precipitation observations. We thank the modeling groups participating in CMIP/PMIP for producing and sharing model output. We thank R. Seager and an anonymous reviewer for their constructive comments; J. Russell, C. Shields, and E. Wahl for helpful discussions; and E. Brady and B. L. Otto-Bliesner for sharing output from the LGM-CO_2 experiment. D. P. L. acknowledges support from the NOAA Hollings Scholarship Program, and C. M. received funding from the NOAA Climate Program Office. All CMIP/PMIP data supporting the conclusions can be obtained from the World Data Center for Climate.

References

Allen, B. D., & Anderson, R. Y. (2000). A continuous, high-resolution record of late Pleistocene climate variability from the Estancia basin, New Mexico. *Geological Society of America Bulletin*, *112*(9), 1444–1458. https://doi.org/10.1130/0016-7606(2000)112%3C1444:ACHRRO%3E2.0.CO;2

Allison, I. S. (1982). *Geology of pluvial Lake Chewaucan, Lake County, Oregon* (79 p.). Corvallis: Oregon State University Press.

Anderson, D. E., & Wells, S. G. (2003). Latest Pleistocene lake highstands in Death Valley, California. In Y. Enzel, S. G. Wells, & N. Lancaster (Eds.), *Paleoenvironments and paleohydrology of the Mojave and southern Great Basin Deserts* (Vol. 368, pp. 115–128). Boulder: Special Paper, Geological Society of America. https://doi.org/10.1130/0-8137-2368-X.115

Antevs, E. (1948). The Great Basin, with emphasis on glacial and post-glacial times—Climate changes and pre-white man. *Bulletin of the University of Utah Biological Series*, *38*, 168–191.

Argus, D. F., & Peltier, W. R. (2010). Constraining models of postglacial rebound using space geodesy: A detailed assessment of model ICE-5G (VM2) and its relatives. *Geophysical Journal International*, *181*, 697–723.

Asmerom, Y., Polyak, V. J., & Burns, S. J. (2010). Variable winter moisture in the southwestern United States linked to rapid glacial climate shifts. *Nature Geoscience*, *3*(2), 114–117. https://doi.org/10.1038/ngeo754

Bacon, S. N., Burke, R. M., Pezzopane, S. K., & Jayko, A. S. (2006). Last Glacial Maximum and Holocene lake levels of Owens Lake, eastern California, USA. *Quaternary Science Reviews*, *25*(11-12), 1264–1282. https://doi.org/10.1016/j.quascirev.2005.10.014

Benson, L. V., Lund, S. P., Burdett, J. W., Kashgarian, M., Rose, T. P., & Schwartz, M. (1998). Correlation of late Pleistocene lake level oscillations in Mono Lake, California, with North Atlantic climate events. *Quaternary Research*, *49*(01), 1–10. https://doi.org/10.1006/qres.1997.1940

Benson, L. V., Smoot, J. P., Lund, S. P., Mensing, S. A., Foit, F. F. Jr., & Rye, R. O. (2013). Insights from a synthesis of old and new climate-proxy data from the Pyramid and Winnemucca lake basins for the period 48 to 11.5 cal ka. *Quaternary International*, *310*, 62–82. https://doi.org/10.1016/j.quaint.2012.02.040

Berger, A. L. (1978). Long-term variations of caloric insolation resulting from the Earth's orbital elements. *Quaternary Research*, *9*(02), 139–167. https://doi.org/10.1016/0033-5894(78)90064-9

Boos, W. R. (2012). Thermodynamic scaling of the hydrological cycle of the Last Glacial Maximum. *Journal of Climate*, *25*(3), 992–1006. https://doi.org/10.1175/JCLI-D-11-00010.1

Braconnot, P., Harrison, S. P., Kageyama, M., Bartlein, P. J., Masson-Delmotte, V., Abe-Ouchi, A., … Zhao, Y. (2012). Evaluation of climate models using palaeoclimatic data. *Nature Climate Change*, *2*(6), 417–424. https://doi.org/10.1038/nclimate1456

Brady, E. C., Otto-Bliesner, B. L., Kay, J. E., & Rosenbloom, N. (2013). Sensitivity to glacial forcing in the CCSM4. *Journal of Climate*, *26*(6), 1901–1925. https://doi.org/10.1175/JCLI-D-11-00416.1

Broecker, W. (2010). Long-term water prospects in the western United States. *Journal of Climate*, *23*(24), 6669–6683. https://doi.org/10.1175/2010JCLI3780.1

COHMAP members (1988). Climatic changes of the last 18,000 years: Observations and model simulations. *Science*, *241*(4869), 1043–1052. https://doi.org/10.1126/science.241.4869.1043

Dallenbach, A., Blunier, T., Fluckiger, J., Stauffer, B., Chappellaz, J., & Raynaud, D. (2000). Changes in the atmospheric CH_4 gradient between Greenland and Antarctica during the last glacial and the transition to the Holocene. *Geophysical Research Letters*, *27*(7), 1005–1008. https://doi.org/10.1029/1999GL010873

Dee, D. P., Uppala, S. M., Simmons, A. J., Berrisford, P., Poli, P., Kobayashi, S., … Vitart, F. (2011). The ERA-Interim reanalysis: Configuration and performance of the data assimilation system. *Quarterly Journal of the Royal Meteorological Society*, *137*(656), 553–597. https://doi.org/10.1002/qj.828

Flückiger, J., Dallenbach, A., Blunier, T., Stauffer, B., Stocker, T. F., Raynaud, D., & Barnola, J.-M. (1999). Variations in atmospheric N_2O concentration during abrupt climatic changes. *Science*, *285*(5425), 227–230. https://doi.org/10.1126/science.285.5425.227

Freidel, D. E. (1993). Chronology and climatic controls of late Quaternary lake-level fluctuations in Chewaucan, Fort Rock, and Alkali basins, south-central Oregon [PhD dissertation], PhD dissertation thesis (244 pp.), University of Oregon.

Giorgetta, M., Jungclaus, J., Reick, C. H., Legutke, S., Bader, J., Böttinger, M., … Stevens, B. (2013). Climate and carbon cycle changes from 1850–2100 in MPI-ESM simulations for the Coupled Model Intercomparison Project phase 5. *Journal of Advances in Modeling Earth Systems*, *5*(3), 572–597. https://doi.org/10.1002/jame.20038

Hevly, R. H. (1985). A 50,000 year record of Quaternary environments, Walker Lake, Cocinino Co., Arizona. In B. F. Jacobs, P. L. Fall, & O. K. Davis (Eds.), *Late Quaternary vegetation and climates of the American Southwest* (pp. 141–154). Dallas, Texas: American Association of Stratigraphic Palynologists Foundation.

Hostetler, S. W., Giorgi, F., Bates, G. T., & Bartlein, P. J. (1994). Lake-atmosphere feedbacks associated with paleolakes Bonneville and Lahontan. *Science*, *263*(5147), 665–668. https://doi.org/10.1126/science.263.5147.665

Hudson, A. M., Quade, J., Ali, G., Boyle, D., Bassett, S., Huntington, K. W., … Wang, X. (2017). Stable C, O and clumped isotope systematics and ^{14}C geochronology of carbonates from the Quaternary Chewaucan closed-basin lake system, Great Basin, USA: Implications for paleoenvironmental reconstructions using carbonates. *Geochimica et Cosmochimica Acta*, *212*, 274–302. https://doi.org/10.1016/j.gca.2017.06.024

Ibarra, D. E., Egger, A. E., Weaver, K. L., Harris, C. R., & Maher, K. (2014). Rise and fall of late Pleistocene pluvial lakes in response to reduced evaporation and precipitation: Evidence from Lake Surprise, California. *Geological Society of America Bulletin*, *126*(11-12), 1387–1415. https://doi.org/10.1130/B31014.1

Kageyama, M., Braconnot, P., Bopp, L., Caubel, A., Foujols, M. A., Guilyardi, E., … Woillez, M. N. (2013). Mid-Holocene and Last Glacial Maximum climate simulations with the IPSL model—Part I: Comparing IPSL_CM5A to IPSL_CM4. *Climate Dynamics*, *40*(9-10), 2447–2468. https://doi.org/10.1007/s00382-012-1488-8

Krider, P. R. (1998). Paleoclimatic significance of late Quaternary lacustrine and alluvial stratigraphy, Animas Valley, New Mexico. *Quaternary Research*, *50*(03), 283–289. https://doi.org/10.1006/qres.1998.1997

Kulongoski, J. T., Hilton, D. R., Izbicki, J. A., & Belitz, K. (2009). Evidence for prolonged El Nino-like conditions in the Pacific during the late Pleistocene: A 43 ka noble gas record from California groundwaters. *Quaternary Science Reviews*, *28*(23-24), 2465–2473. https://doi.org/10.1016/j.quascirev.2009.05.008

Lachniet, M. S., Denniston, R. F., Asmerom, Y., & Polyak, V. (2014). Orbital control of western North America atmospheric circulation and climate over two glacial cycles. *Nature Communications*, *5*, 1–8.

Lambeck, K., Purcell, A., Zhao, J., & Svensson, N.-O. (2010). The Scandinavian Ice Sheet: From MIS4 to the end of the Last Glacial Maximum. *Boreas*, *39*(2), 410–435. https://doi.org/10.1111/j.1502-3885.2010.00140.x

Lau, W. K. M., & Kim, K.-M. (2015). Robust Hadley circulation changes and increasing global dryness due to CO_2 warming from CMIP5 model projections. *Proceedings of the National Academy of Sciences*, *112*, 3630–3635.

Li, L., Lin, P., Yu, Y., Wang, B., Zhou, T., Liu, L., … Qiao, F. (2013). The flexible global ocean-atmosphere-land system model, Grid-point version 2: FGOALS-g2. *Advances in Atmospheric Sciences*, *30*(3), 543–560. https://doi.org/10.1007/s00376-012-2140-6

Lin, J. C., Broecker, W. S., Hemming, S. R., Hajdas, I., Anderson, R. F., Smith, G. I., … Bonani, G. (1998). A reassessment of U-Th and ^{14}C ages for late-glacial high-frequency hydrological events at Searles Lake, California. *Quaternary Research*, *49*(01), 11–23. https://doi.org/10.1006/qres.1997.1949

Livneh, B., Rosenberg, E. A., Lin, C., Nijssen, B., Mishra, V., Andreadis, K. M., … Lettenmaier, D. P. (2013). A long-term hydrologically based dataset of land surface fluxes and states for the conterminous United States: Update and extensions. *Journal of Climate*, *26*(23), 9384–9392. https://doi.org/10.1175/JCLI-D-12-00508.1

Long, A. (1966). Late Pleistocene and recent chronologies of Playa Lakes in Arizona and New Mexico, (141 pp.). Tucson, Arizona: University of Arizona.

Lora, J. M., Mitchell, J. L., Risi, C., & Tripati, A. E. (2017). North Pacific atmospheric rivers and their influence on western North America at the Last Glacial Maximum. *Geophysical Research Letters*, *44*, 1051–1059. https://doi.org/10.1002/2016GL071541

Lora, J. M., Mitchell, J. L., & Tripati, A. E. (2016). Abrupt reorganization of North Pacific and western North American climate during the last deglaciation. *Geophysical Research Letters*, *43*, 11,796–11,804. https://doi.org/10.1002/2016GL071244

Lyle, M., Heusser, L., Ravelo, C., Yamamoto, M., Barron, J., Diffenbaugh, N. S., … Andreasen, D. (2012). Out of the tropics: The Pacific, Great Basin lakes, and late Pleistocene water cycle in the western United States. *Science*, *337*(6102), 1629–1633. https://doi.org/10.1126/science.1218390

Maher, K., Ibarra, D. E., Oster, J. L., Miller, D. M., Redwine, J. L., Reheis, M. C., & Harden, J. W. (2014). Uranium isotopes in soils as a proxy for past infiltration and precipitation across the western United States. *American Journal of Science*, *314*(4), 821–857. https://doi.org/10.2475/04.2014.01

Markgraf, V., Bradbury, J. P., Forester, R. M., Singh, G., & Sternberg, R. S. (1984). San Agustin Plains, New Mexico: Age and paleoenvironmental potential reassessed. *Quaternary Research*, *22*(03), 336–343. https://doi.org/10.1016/0033-5894(84)90027-9

McGee, D., Quade, J., Edwards, R. L., Broecker, W. S., Cheng, H., Reiners, P. W., & Evenson, N. (2012). Lacustrine cave carbonates: Novel archives of paleohydrologic change in the Bonneville Basin (Utah, USA). *Earth and Planetary Science Letters*, *351-352*, 182–194. https://doi.org/10.1016/j.epsl.2012.07.019

Mifflin, M. D., & Wheat, M. M. (1979). Pluvial lakes and estimated pluvial climates of Nevada, (52 pp.).

Monnin, E., Indermuhle, A., Dallenbach, A., Fluckinger, J., Stauffer, B., Stocker, T. F., … Barnola, J.-M. (2001). Atmospheric CO_2 concentrations over the last glacial termination. *Science*, *291*(5501), 112–114. https://doi.org/10.1126/science.291.5501.112

Munroe, J. S., & Laabs, B. J. C. (2013). Temporal correspondence between pluvial lake highstands in the southwestern US and Heinrich Event 1. *Journal of Quaternary Science*, *28*(1), 49–58. https://doi.org/10.1002/jqs.2586

Musgrove, M., Banner, J. L., Mack, L. E., Combs, D. M., James, E. W., Cheng, H., & Edwards, R. L. (2001). Geochronology of late Pleistocene to Holocene speleothems from central Texas: Implications for regional paleoclimate. *Geological Society of America Bulletin*, *113*(12), 1532–1543. https://doi.org/10.1130/0016-7606(2001)113%3C1532:GOLPTH%3E2.0.CO;2

Newman, M., Kiladis, G. N., Weickmann, K. M., Ralph, F. M., & Sardeshmukh, P. D. (2012). Relative contributions of synoptic and low-frequency eddies to time-mean atmospheric moisture transport, including the role of atmospheric rivers. *Journal of Climate*, *25*(21), 7341–7361. https://doi.org/10.1175/JCLI-D-11-00665.1

Orme, A. J. (2008). Lake Thompson, Mojave Desert, California: The late Pleistocene lake system and its Holocene desiccation. In M. C. Reheis, R. Hershler, & D. M. Miller (Eds.), *Late Cenozoic drainage history of the southwestern Great Basin and lower Colorado River region: Geologic and biotic perspectives*, *Geological Society of America Special Paper* (Vol. 439, pp. 261–278). The Geological Society of America. https://doi.org/10.1130/2008.2439(11)

Orme, A. R., & Orme, A. J. (2008). Late Pleistocene shorelines of Owens Lake, California, and their hydroclimatic and tectonic implications. In M. C. Reheis, R. Hershler, & D. M. Miller (Eds.), *Late Cenozoic drainage history of the southwestern Great Basin and lower Colorado River region: Geologic and biotic perspectives*, *Geological Society of America Special Paper* (Vol. 439, pp. 207–225). Geological Society of America. https://doi.org/10.1130/2008.2439(09)

Oster, J. L., Ibarra, D. E., Winnick, M. J., & Maher, K. (2015). Steering of westerly storms over western North America at the Last Glacial Maximum. *Nature Geoscience*, *8*(3), 201–205. https://doi.org/10.1038/ngeo2365

Otto-Bliesner, B. L., & Clement, A. (2005). The sensitivity of the Hadley circulation to past and future forcings in two climate models. In H. F. Diaz, & R. S. Bradley (Eds.), *The Hadley circulation: Present, past and future* (pp. 437–464). Dordrecht, The Netherlands: Kluwer Academic Publishers.

Oviatt, C. G. (2015). Chronology of Lake Bonneville, 30,000 to 10,000 yr B.P. *Quaternary Science Reviews*, *110*, 166–171. https://doi.org/10.1016/j.quascirev.2014.12.016

Oviatt, C. G., Thompson, R. S., Kaufman, D. S., Bright, J., & Forester, R. M. (1999). Reinterpretation of the Burmester Core, Bonneville Basin, Utah. *Quaternary Research*, *52*(02), 180–184. https://doi.org/10.1006/qres.1999.2058

Pound, M. J., Tindall, J., Pickering, S. J., Haywood, A. M., Dowsett, H. J., & Salzmann, U. (2014). Late Pliocene lakes and soils: A global data set for the analysis of climate feedbacks in a warmer world. *Climate of the Past*, *10*(1), 167–180. https://doi.org/10.5194/cp-10-167-2014

Quade, J., & Broecker, W. S. (2009). Dryland hydrology in a warmer world: Lessons from the last glacial period. *European Physical Journal Special Topics*, *176*(1), 21–36. https://doi.org/10.1140/epjst/e2009-01146-y

Quade, J., Forester, R. M., & Whelan, J. F. (2003). Late Quaternary paleohydrologic and paleotemperature change in southern Nevada. *Geological Society of America Special Papers*, *368*, 165–188.
Reheis, M. C., Adams, K. D., Oviatt, C. G., & Bacon, S. N. (2014). Pluvial lakes in the Great Basin of the western United States—A view from the outcrop. *Quaternary Science Reviews*, *97*, 33–57. https://doi.org/10.1016/j.quascirev.2014.04.012
Reimer, P. J., Bard, E., Bayliss, A., Beck, J. W., Blackwell, P. G., Ramsey, C. B., … van der Plicht, J. (2013). IntCal13 and Marine13 radiocarbon age calibration curves 0–50,000 years cal BP. *Radiocarbon*, *55*(04), 1869–1887. https://doi.org/10.2458/azu_js_rc.55.16947
Seager, R., & Henderson, N. (2013). Diagnostic computation of moisture budgets in the ERA-Interim reanalysis with reference to analysis CMIP-archived atmospheric model data. *Journal of Climate*, *26*(20), 7876–7901. https://doi.org/10.1175/JCLI-D-13-00018.1
Seager, R., Naik, N., & Vecchi, G. A. (2010). Thermodynamic and dynamic mechanisms for large-scale changes in the hydrologic cycle in response to global warming. *Journal of Climate*, *23*(17), 4651–4668. https://doi.org/10.1175/2010JCLI3655.1
Seager, R., Neelin, D., Simpson, I., Liu, H., Henderson, N., Shaw, T., … Cook, B. (2014). Dynamical and thermodynamical causes of large-scale changes in the hydrological cycle over North America in response to global warming. *Journal of Climate*, *27*(20), 7921–7948. https://doi.org/10.1175/JCLI-D-14-00153.1
Seager, R., Ting, M., Held, I., Kushnir, Y., Lu, J., Vecchi, G., … Naik, N. (2007). Model projections of an imminent transition to a more arid climate in southwestern North America. *Science*, *316*(5828), 1181–1184. https://doi.org/10.1126/science.1139601
Stuiver, M., & Reimer, P. J. (1993). Extended C-14 database and revised CALIB 3.0 C-14 age calibration program. *Radiocarbon*, *35*(01), 215–230. https://doi.org/10.1017/S0033822200013904
Sutton, R. T., Dong, B., & Gregory, J. M. (2007). Land/sea warming ratio in response to climate change: IPCC AR4 model results and comparison with observations. *Geophysical Research Letters*, *34*, L02701. https://doi.org/10.1029/2006GL028164
Szabo, B. J., Kolesar, P. T., Riggs, A. C., Winograd, I. J., & Ludwig, K. R. (1994). Paleoclimatic inferences from a 120,000-yr calcite record of water-table fluctuation in Browns Room of Devils Hole, Nevada. *Quaternary Research*, *41*(01), 59–69. https://doi.org/10.1006/qres.1994.1007
Tarasov, L., & Peltier, W. R. (2004). A geophysically constrained large ensemble analysis of the deglacial history of the North American ice-sheet complex. *Quaternary Science Reviews*, *23*(3-4), 359–388. https://doi.org/10.1016/j.quascirev.2003.08.004
Ullman, D. J., LeGrande, A. N., Carlson, A. E., Anslow, F. S., & Licciardi, J. M. (2013). Assessing the impact of Laurentide Ice-Sheet topography on glacial climate. *Climate of the Past Discussion*, *9*(3), 3239–3306. https://doi.org/10.5194/cpd-9-3239-2013
Voldoire, A., Sanchez-Gomez, E., Salas y Mélia, D., Decharme, B., Cassou, C., Sénési, S., … Chauvin, F. (2013). The CNRM-CM5.1 global climate model: Description and basic evaluation. *Climate Dynamics*, *40*(9-10), 2091–2121. https://doi.org/10.1007/s00382-011-1259-y
Wagner, J. D. M., Cole, J. E., Beck, J. W., Patchett, P. J., Henderson, G. M., & Barnett, H. R. (2010). Moisture variability in the southwestern United States linked to abrupt glacial climate change. *Nature Geoscience*, *3*(2), 110–113. https://doi.org/10.1038/ngeo707
Watanabe, S., Hajima, T., Sudo, K., Nagashima, T., Takemura, T., Okajima, H., … Kawamiya, M. (2011). MIROC-ESM 2010: Model description and basic results of CMIP5-20c3m experiments. *Geoscientific Model Development*, *4*(4), 845–872. https://doi.org/10.5194/gmd-4-845-2011
Waters, M. R. (1989). Late Quaternary lacustrine history and paleoclimatic significance of pluvial Lake Cochise, southeastern Arizona. *Quaternary Research*, *32*(01), 1–11. https://doi.org/10.1016/0033-5894(89)90027-6
Wei, W., & Lohmann, G. (2012). Simulated Atlantic multidecadal oscillation during the Holocene. *Journal of Climate*, *25*(20), 6989–7002. https://doi.org/10.1175/JCLI-D-11-00667.1
Wells, S. G., Brown, W. J., Enzel, Y., Anderson, R. Y., & McFadden, L. D. (2003). Late Quaternary geology and paleohydrology of pluvial Lake Mojave, southern California. In Y. Enzel Y, S.G. Wells, & N. Lancaster (Eds.), *Paleoenvironments and paleohydrology of the Mojave and southern Great Basin Deserts*, *Geological Society of America Special Paper* (Vol. 368, pp 79–114). The Geological Society of America. https://doi.org/10.1130/0-8137-2368-X.79
Wilkins, D. E., & Currey, D. R. (1997). Timing and extent of late Quaternary paleolakes in the Trans-Pecos closed basin, west Texas and south-central New Mexico. *Quaternary Research*, *47*, 306–315. https://doi.org/10.1006/qres.1997.1896
Wills, R. C., Byrne, M. P., & Schneider, T. (2016). Thermodynamic and dynamic controls on changes in the zonally anomalous hydrological cycle. *Geophysical Research Letters*, *43*, 4640–4649. https://doi.org/10.1002/2016GL068418
Wong, C. I., Potter, G. L., Montanez, I. P., Otto-Bliesner, B. L., Behling, P., & Oster, J. L. (2016). Evolution of moisture transport to the western U.S. during the last deglaciation. *Geophysical Research Letters*, *43*, 3468–3477. https://doi.org/10.1002/2016GL068389
Yanase, W., & Abe-Ouchi, A. (2010). A numerical study on the atmospheric circulation over the midlatitude North Pacific during the Last Glacial Maximum. *Journal of Climate*, *23*(1), 135–151. https://doi.org/10.1175/2009JCLI3148.1
Yoshimori, M., Yokohata, T., & Abe-Ouchi, A. (2009). A comparison of climate feedback strength between CO_2 doubling and LGM experiments. *Journal of Climate*, *22*(12), 3374–3395. https://doi.org/10.1175/2009JCLI2801.1
Yukimoto, S., Adachi, Y., Hosaka, M., Sakami, T., Yoshimura, H., Hirabara, M., … Kitoh, A. (2012). A new global climate model of the Meteorological Research Institute: MRI-CGCM3. *Journal of the Meteorological Society of Japan*, *90A*, 23–64. https://doi.org/10.2151/jmsj.2012-A02
Zhu, C., Waddell, R. K. Jr., Star, I., & Ostrander, M. (1998). Responses of ground water in the Black Mesa basin, northeastern Arizona, to paleoclimatic changes during the late Pleistocene and Holocene. *Geology*, *26*(2), 127–130. https://doi.org/10.1130/0091-7613(1998)026%3C0127:ROGWIT%3E2.3.CO;2